Numerical modelling of interfacial soil erosion with viscous incompressible flows

Golay Frédéric[a,b], Lachouette Damien[a,b], Bonelli Stéphane[b], Seppecher Pierre[a]

(a) Institut de Mathématique de Toulon, Université du Sud Toulon – Var, France

(b) Unité de recherche Ouvrages Hydrauliques et Hydrologie, Cemagref, Aix-en-Provence, France

Keywords: Erosion, finite volume, penalization, level set, interface, fictitious domain

Corresponding author:
Dr. Frédéric Golay
E-mail address: frederic.golay@univ-tln.fr

Abstract: The aim of this study is to develop a numerical model for simulating surface erosion occurring at a fluid/soil interface subject to a flow process. Balance equations with jump relations are used. A penalization procedure including a fictitious domain method is used to compute the Stokes flow around obstacles, in order to avoid body-fitted unstructured meshes and instead use fast and efficient finite volume approximations on Cartesian meshes. The evolution of the water/soil interface is described by using a Level Set function. The ability of the model to predict the interfacial erosion of soils is confirmed by several numerical simulations.

1 INTRODUCTION

The literature provides many examples of modelling soil erosion linked to sediment transport and the hydraulics of free-surface flows. However, most of these studies have taken a global approach: water flow is expressed in terms of average velocity in the framework of shallow water equations; erosion is driven by the flow's capacity to transport particles rather than by a process of particle removal caused by the flow. Also, the precise description of interface behaviour has been more or less neglected.

Several models of the erosion of a sand layer under axial and radial flow conditions have been proposed in the framework of the continuum theory of mixtures [22, 30, 31]. In these studies, the erosion process is assumed to involve a smooth transition from solid-like to fluid-like behaviour. This transition is described by a three-phase model (comprising solid, fluid, and fluidized phases). The interactions of these three phases are constrained by balance equations. A source term is introduced into mass balance equations to describe the detachment and exchange of sand particles via an erosion law.

A recent model proposed by Chauchat and Médale [8] involves a smooth transition from solid-like to fluid-like behaviour with a two-phase model (granular and fluid phases). In this case, the erosion process is the result of momentum exchange between the phases in question, which leads to source terms in the momentum balance equations. The key point in these approaches is that the erosion process is driven by the flow of water within the soil, i.e. the Darcy-Brinkman flow. These models are therefore relevant for permeable soils such as granular media. However, most cohesive soils like clay exhibit very low permeability and the internal flow generated by an external flow is likely to be neglected in these soils.

The philosophy underlying the present approach differs from previous theories of surface erosion in that our description deals with singular (or discontinuous) fluid/soil interfaces [3, 5], rather than with smooth fluid/soil interfaces. The aim here is to model as simply as possible the erosion of a cohesive soil generated by a flow of water tangential to the soil/water interface. These results were announced in [15].

The paper is organized as follows: Section 2 summarizes the governing equations for the fluid flow and for the evolution of the fluid/soil interface. In Section 3, a penalized model (fictitious domains) is introduced, leading to a unified formulation for the equations for the whole domain (fluid and soil). Section 4 describes the numerical implementation of the model. Finally, Section 5 presents a validation of the model and some illustrative examples.

2 GOVERNING EQUATIONS

We study the surface erosion of a fluid/soil interface subjected to a flow running parallel to the interface. The soil is eroded by the flow which then carries away the particles removed from the surface of the soil. The basic balance equations and the erosion constitutive law developed by Bonelli and Brivois [3, 5] are used. The quantity of particles present in the fluid is assumed here to be small enough not to significantly affect the properties of the carrier fluid: this is the dilute suspension flow assumption. For the sake of simplicity, neither the gravitational forces nor the sedimentation and deposition processes are considered. In the fluid domain, denoted Ω_f, $\mathbf{u}$ denotes fluid velocity, ρ_f constant fluid density, μ_f fluid viscosity, p fluid pressure, and $\mathbf{T}$ Cauchy stress in the fluid. The equations describing an incompressible viscous flow are the mass and momentum balance equations given by:

$$\nabla \cdot \mathbf{u} = 0 \tag{1}$$

$$\rho_f \left[\frac{\partial \mathbf{u}}{\partial t} + (\mathbf{u} \cdot \nabla)\mathbf{u} \right] = \nabla \cdot \mathbf{T} \tag{2}$$

$$\mathbf{T} = 2\mu_f \, e^D\left(\mathbf{u}\right) - p \, \mathbf{I} \tag{3}$$

where $e^D\left(\mathbf{u}\right)$ denotes the deviatoric part of the rate-of-strain tensor $e\left(\mathbf{u}\right) = (\nabla\mathbf{u} + \nabla^T\mathbf{u}) \,/\, 2$, $e^D\left(\mathbf{u}\right) = e\left(\mathbf{u}\right) - \left(1 \,/\, 3\right) tr\left(e\left(\mathbf{u}\right)\right)\mathbf{I}$. The distinction between $e\left(\mathbf{u}\right)$ and $e^D\left(\mathbf{u}\right)$, clearly useless here because of Eq. (1), will be essential later.

We denote the fluid/soil interface as Γ. Due to the erosion process, a mass flux crosses Γ. As a result, Γ may move and is not a material surface: Γ is not defined by the same particles at different times. We emphasize the fact that, in our description, Γ is a purely geometric separating surface with no thickness.

Our description of the soil is a simplified one. We assume it to be saturated and motionless. Any particle in the soil, whether a fluid or solid, has a negligible velocity ($\mathbf{u}_s = 0$). It is also assumed

that, at our macroscopic level of description, soil density ρ_s is uniform and constant. Since this soil is saturated and devoid of seepage, the mass flux crossing the interface is an erosion flux.

Mass and momentum balance lead to jump equations across Γ. Let us denote as $\mathbf{n}$ the unit vector normal to Γ oriented from the fluid toward the soil, and $\mathbf{c}_\Gamma$ the normal celerity vector of Γ. The mass balance at the interface is written as:

$$\rho_s(\mathbf{c}_\Gamma - \mathbf{u}_{is}) \cdot \mathbf{n} = \rho_f(\mathbf{c}_\Gamma - \mathbf{u}_{if}) \cdot \mathbf{n}\,. \tag{4}$$

where $\mathbf{u}_{is}$ and $\mathbf{u}_{if}$ stand for the limit values of $\mathbf{u}$ on the solid and fluid sides of the interface respectively. Taking into account that $\mathbf{u}_s = 0$, Equation (4) can be reformulated in the following form the interest of which will appear later:

$$\rho_f\left(\mathbf{u}_{if} \cdot \mathbf{n} - \mathbf{u}_{is} \cdot \mathbf{n}\right) = \left(\rho_f - \rho_s\right)\mathbf{c}_\Gamma \cdot \mathbf{n}\,. \tag{5}$$

The total flux of material (both particles and water) crossing the interface can be defined by:

$$\dot{m} = \rho_f(\mathbf{c}_\Gamma - \mathbf{u}_{if}) \cdot \mathbf{n} = \rho_s \mathbf{c}_\Gamma \cdot \mathbf{n} \tag{6}$$

The momentum balance at the interface gives:

$$\sigma_{if} - \sigma_{is} = \dot{m}^2\left(\frac{1}{\rho_f} - \frac{1}{\rho_s}\right),\ \boldsymbol{\tau}_{if} - \boldsymbol{\tau}_{is} = \dot{m}\mathbf{v}_{if}\,. \tag{7}$$

where $\sigma = \mathbf{n} \cdot \mathbf{T} \cdot \mathbf{n}$ is the normal stress, $\boldsymbol{\tau} = \mathbf{T} \cdot \mathbf{n} - \sigma\mathbf{n}$ is the tangential stress vector and $\mathbf{v} = \mathbf{u} - (\mathbf{u} \cdot \mathbf{n})\mathbf{n}$ is the tangential velocity.

We assume that the tangential velocities are continuous across Γ (a constitutive assumption usually called the “no-slip condition at the interface”): $\mathbf{v}_{if} = 0$. Therefore, on the basis of (7), we know that the tangential stress $\boldsymbol{\tau}$ is continuous across Γ. Note that the normal stress may be discontinuous across Γ.

Since a tangential flow is dealt with, a threshold constitutive law [3, 5] is used for soil erosion:

$$\dot{m} = \begin{cases} k_{er}(\left|\boldsymbol{\tau}_{if}\right| - \tau_c) \text{ if } \left|\boldsymbol{\tau}_{if}\right| > \tau_c \\ 0 \text{ otherwise} \end{cases}. \tag{8}$$

Threshold τ_c is referred to as the critical shear stress and $k_{er} > 0$ as the coefficient of soil erosion.

3 MATHEMATICAL MODEL

3.1 Fictitious domain

The aim here is to simulate a fluid flow with a moving boundary Γ. A classical method consists in building a mesh of the fluid part with cell edges belonging to Γ. It is necessary to regularly adapt the mesh or remesh as the boundary varies. This numerical process can become prohibitive, especially when considering a three-dimensional problem. That is why a spatial discretization that is not fitted to the interface is used. This method is called the "fictitious domain method" or "penalized method". The main idea of this approach consists in solving the fluid flow problem in a bigger fixed domain instead of the moving fluid domain. This method is popular because it allows the use of fairly structured meshes. The fictitious domain method is now widely used (in particular for fluid-porous-solid flows) and has been mathematically justified (see e.g. [1, 2, 4, 11, 18, 25]).

Let $\Omega = \Omega_f \cup \Omega_s$ be a fluid/solid domain with boundary $\partial\Omega$. The penalized method allows describing the behaviour of the two sub-domains by equations valid for the whole domain by introducing a new term in the momentum balance equation:

$$\rho_f \left[\frac{\partial \mathbf{u}}{\partial t} + (\mathbf{u} \cdot \nabla)\mathbf{u} \right] - \nabla \cdot \left[2\mu_f e^D(\mathbf{u}) \right] = -\nabla p - \frac{\mu_f H}{K_s} \mathbf{u} \,. \tag{9}$$

The penalization coefficient K_s is a very small number that has the dimension of a geometric permeability and H is the characteristic function of the soil domain (which is unity within Ω_s and zero elsewhere). As the last term of the right-hand side of Equation (9) is zero in the fluid domain, the equation reduces to the Navier-Stokes equation. In the soil domain, the penalization leads to a very low velocity $\mathbf{u}$ and the left-hand side of Eq. (9) is negligible.

Note that mass balance equations (1) and (5) (together with the implicit equation $\nabla \cdot \mathbf{u}_s = 0$ valid in the soil) can be summarized in the following equation valid for the whole domain:

$$\nabla \cdot \left(\rho_f \mathbf{u} \right) = (\rho_s - \rho_f)\mathbf{c}_\Gamma \cdot DH \,. \tag{10}$$

Note that as H is the characteristic function of the soil domain, DH is a measure concentrated on the interface and the right hand side is a mass source term at the interface.

Equations (9) and (10) must be understood in the sense of distributions. Indeed, singularities occur on the interface. Here the fact that only the deviatoric part of the rate-of-strain tensor appears in (9) is essential. Otherwise, no mass transfer would be possible.

3.2 Determination of the interface by the Level Set Method

The Level Set method is an appropriate formulation for considering sharp interface. It consists in introducing a function ψ that is negative in the fluid domain Ω_f and positive in the soil domain Ω_s. Interface Γ is represented by the zero level set of ψ. A possible and relevant approach is to choose this function as the signed distance to the interface. The motion of the interface is thus determined by the evolution of function ψ. Keeping track of the whole function ψ while only its zero level set is relevant may appear inefficient, but it in fact simplifies both the mathematical formulation and numerical implementation.

This approach can be considered as a front capturing method as no explicit information on the interface is required during the computational process; the interface is recovered at the end of computation by locating the zero level. Cartesian meshes are used because capturing methods do not require body-fitted grids instead of front tracking methods. The accuracy of the definition of the interface strongly depends on the numerical scheme applied to the transport equation.

This Level Set formulation was introduced by Other and Sethian ([21]) and is widely used for multi-fluid flows (e.g. [6, 20, 27]), with a fictitious domain approach (e.g. [7]) in both two and three-dimensional cases (e.g. [24]).

Assuming that the zero level set of ψ and the interface coincide at $t = 0$, then they must coincide at all times provided that ψ satisfies $\partial\psi / \partial t + \mathbf{c}_\Gamma \cdot \nabla\psi = 0$ at the interface. This condition is automatically satisfied assuming that ψ is then driven by a transport equation:

$$\frac{\partial\psi}{\partial t} + \mathbf{c} \cdot \nabla\psi = 0 \tag{11}$$

where $\mathbf{c}$ is an extension on the whole domain of the interface celerity $\mathbf{c}_\Gamma$ defined on the interface in (4) .

Note that the normal to the interface is given by the gradient of the level set function:

$$\mathbf{n} = \frac{\nabla\psi}{\|\nabla\psi\|} \tag{12}$$

As the level set function ψ is defined in the whole domain, vector $\mathbf{n}$ is also defined in the whole domain. This enables us to extend the interface celerity along the lines of field $\mathbf{n}$, by considering $\mathbf{c}\left(\mathbf{x}\right) = \hat{\mathbf{c}}\left(\mathbf{x}, T^*\right)$, where $\hat{\mathbf{c}}$ is the solution on $\left[0, T^*\right]$ of the following fictitious transport equation (with fictitious time t^*):

$$\frac{\partial\hat{\mathbf{c}}}{\partial t^*} + \mathrm{sgn}(\psi)\,\mathbf{n} \cdot \nabla\hat{\mathbf{c}} = \mathbf{0} \tag{13}$$

with the condition:

$$\hat{\mathbf{c}}\left(\mathbf{x}, t^*\right) = \mathbf{c}_\Gamma\left(\mathbf{x}\right) \quad if\ \mathbf{x} \in \Gamma(t) \tag{14}$$

Remark: In order to avoid computation oscillation near the interface, (13) is solved in two steps: first in the soil domain and then in the fluid domain.

3.3 Assumption of slow erosion

Let us now check what the important physical parameters of the problem are. Let ℓ_f be a characteristic length scale of the domain and V_f the reference fluid velocity. By introducing the dimensionless variables $\tilde{\mathbf{u}} = \mathbf{u} / V_f$, $\tilde{p} = p / V_f^2\rho_f$, $\tilde{\tau} = \tau / \rho_f V_f^2$, $\tilde{\mathbf{c}} = \rho_s\mathbf{c} / V_f^2 k_{er}\rho_f$ and the

dimensionless operators $\tilde{\nabla} = \ell_f \nabla$, $\partial / \partial \tilde{t} = \ell_f \partial / V_f \partial t$ the system of equations (8)-(11) that has to be solved is:

$$\widetilde{div}\ \tilde{\mathbf{u}} = \boldsymbol{\mathcal{D}}_m \boldsymbol{\mathcal{E}}_r \tilde{\mathbf{c}} \cdot \tilde{D} H \tag{15}$$

$$\frac{\partial \tilde{\mathbf{u}}}{\partial \tilde{t}} + (\tilde{\mathbf{u}} \cdot \tilde{\nabla})\tilde{\mathbf{u}} - \frac{1}{R_e} \tilde{\nabla} \cdot \left[2\, \tilde{e}^D(\tilde{\mathbf{u}}) \right] = -\tilde{\nabla} \tilde{p} - \frac{H}{\boldsymbol{\mathcal{K}}_p} \tilde{\mathbf{u}}\,. \tag{16}$$

$$H = \begin{cases} 1 \text{ if } \psi > 0, \\ 0 \text{ otherwise} \end{cases} \tag{17}$$

$$\frac{\partial \psi}{\partial \tilde{t}} + \boldsymbol{\mathcal{E}}_r\ \tilde{\mathbf{c}} \cdot \tilde{\nabla} \psi = 0 \tag{18}$$

$$\tilde{\mathbf{c}} \cdot \mathbf{n} = \begin{cases} \left| \tilde{\boldsymbol{\tau}}_{if} \right| - \tilde{\tau}_c \text{ if } \left| \tilde{\boldsymbol{\tau}}_{if} \right| > \tilde{\tau}_c \text{ on } \Gamma \\ 0 \text{ otherwise} \end{cases} \tag{19}$$

where $R_e = \rho_f \ell_f V_f \,/\, \mu_f$ is the Reynolds number, $\boldsymbol{\mathcal{K}}_p = \rho_f V_f K_s \,/\, \ell_f \mu_f$ is the penalization number, $\boldsymbol{\mathcal{D}}_m = \left(\rho_s - \rho_f \right) / \rho_f$ is the relative density ratio and $\boldsymbol{\mathcal{E}}_r = V_f k_{er} \rho_f \,/\, \rho_s$ is the erosion number.

One of these four dimensionless parameters (not counting the dimensionless threshold $\tilde{\tau}_c$), is a purely mathematical artefact: $\boldsymbol{\mathcal{K}}_p \ll 1$ in order to recover an impervious fixed soil. The number $\boldsymbol{\mathcal{D}}_m$ is of order one and does not play an essential role. The erosion number $\boldsymbol{\mathcal{E}}_r$ is the ratio of the characteristic time of the flow compared to the characteristic time of the erosion process. In most practical cases the ratio is extremely small ($\boldsymbol{\mathcal{E}}_r \ll 1$). This leads to a major simplification of the problem. Indeed, from (18), we deduce that ψ is quasi constant at the time scale of the flow.

This implies that there is no time dependent source term in (16). When the boundary conditions are stationary, it is possible to search for an incompressible stationary (or quasi-steady) solution for (16). The time scales of the flow and of the erosion process are so different that the system of equations can be split: for a given ψ a stationary solution of the Navier Stokes equation is sought, omitting the erosion process. This provides the shear stress on the boundary from which we deduce

the interface celerity and then the evolution of ψ. If we also assume that $R_e \ll 1$, the Navier Stokes equation is reduced to the Stokes equation. The influence of both the concentration of soil particles in the flow and the inertial effects can be neglected, and the flow is quasi-steady. This is consistent with our assumption of a dilute suspension flow.

The case of turbulent flows, for which the orders of magnitude are different, is beyond the scope of this paper. An initial study of erosion due to a turbulent flow was performed in [3] and [19] in the particular 1D-case of a turbulent piping flow.

4 NUMERICAL MODELING

4.1 General procedure

As the erosion process is much slower than the main fluid flow, the two phenomena are split.

The algorithm is organized as follows:

a) Define a Level Set function ψ_0 representing the interface at initial time t_0.

   Define the initial flow $\left(\mathbf{u}_0, p_0\right)$.

b) Define the time step δt for the erosion process.

c) Compute the interface celerity in terms of $\left(\mathbf{u}_n, p_n\right)$

d) Compute the new value ψ_{n+1} at time $t_{n+1} = t_n + \delta t$ by solving the transport equation (11). Apply a redistancing procedure on ψ_{n+1}, if needed.

e) Solve the Stokes equations in order to update $\left(\mathbf{u}_{n+1}, p_{n+1}\right)$.

f) Iterate (b)-(e) for each time step.

4.2 The Stokes solver

At time t_n, with the soil position being given by ψ_n, the stationary mass and penalized momentum balance equations (1), (9) are solved, in order to obtain the velocity and pressure fields $\left(\mathbf{u}_n, p_n\right)$. In

what follows each quantity indexed by *n* refers to time t_n. Then the following Stokes equations are written:

$$\nabla \cdot \mathbf{u}_n = 0 \tag{20}$$

$$\nabla \cdot \left[\mu_f (\nabla \mathbf{u}_n + \nabla^T \mathbf{u}_n) \right] - \frac{\mu_f H(\psi_n)}{K_s} \mathbf{u}_n - \nabla p_n = 0 \tag{21}$$

In order to deal with the constraint of divergence-free velocity, we use the Augmented Lagrangian method (see e.g. [13, 34, 14]), which is similar to the artificially compressible method introduced by [9, 28]. This predictor/corrector iterative method consists in solving a sequence of unconstrained problems that converge towards a solution which satisfies the incompressibility constraint. The iterations of the Augmented Lagrangian method, indexed by superscript k, are repeated until a numerical threshold controlling the constraint is reached. No boundary conditions are needed for the pressure. By denoting $(\mathbf{u}_n^k, p_n^k)$ the velocity and the pressure fields at time t_n and iteration *k* of the Augmented Lagrangian method, the algorithm to be solved (20)-(21) is as follows:

(1) Initialize $(\mathbf{u}_n^0, p_n^0) = (\mathbf{u}_{n-1}, p_{n-1})$

(2) Solve the following linear system for $\mathbf{u}_n^k$

$$\nabla \cdot \left[\mu_f (\nabla \mathbf{u}_n^k + \nabla^T \mathbf{u}_n^k) \right] - r_1 \nabla \left(\nabla \cdot \mathbf{u}_n^k \right) - \frac{\mu_f H(\psi)}{K_s} \mathbf{u}_n^k = \nabla p_n^{k-1} \tag{22}$$

(3) Update pressure $\mathrm{p}_\mathrm{n}^\mathrm{k}$ by using

$$p_n^k = p_n^{k-1} - r_2 \nabla \cdot \mathbf{u}_n^k \tag{23}$$

(4) Increase *k* and iterate (2)-(3) until criterion $\left| \nabla \cdot \mathbf{u}_n^k \right| \leq \varepsilon$ is satisfied

(5) Assign $(\mathbf{u}_n, p_n) = (\mathbf{u}_n^k, p_n^k)$.

Here, ε denotes the desired convergence tolerance. The quantities r_1 and r_2 are the coefficients of the method; the particular case $r_1 = r_2$ corresponds to the standard Augmented Lagrangian method. These coefficients can be chosen in an adaptive way as in [35].

For the spatial discretization of (22) and (23), we use a finite volume method on a Cartesian staggered grid initially developed by Harlow and Welch [16] (Marker and Cell method, MAC) and now widely used in many applications (see e.g. [10, 23, 32, 33]). For the sake of simplicity, the formulation in the 2D case is presented here, but the 3D case does not involve additional difficulty and the subscript *n* is dropped. Space discretizations in the directions x and y are denoted $\triangle x$ and $\triangle y$ respectively. Pressure $p_{i,j}$ is defined at the centre $X_{i,j} = (x_i, y_j)$ of the cell (i,j), while the horizontal velocity $u_{i,j}$ is defined at the middle $X_{i-1/2,j}$ of the vertical left-hand edge of the cell and the vertical velocity $v_{i,j}$ is defined at the middle $X_{i,j-1/2}$ of the bottom horizontal edge of the cell (Figures 1 and 2).

$$u_{i,j} = u(x_{i-1/2}, y_j)\ ; \quad v_{i,j} = v(x_i, y_{j-1/2})\ ; \quad p_{i,j} = p(x_i, y_j) \tag{24}$$

Using this notation, equation (23) is discretized in

$$p_{i,j}^k = p_{i,j}^{k-1} - r_2 \left(\frac{u_{i+1,j}^k - u_{i,j}^k}{\Delta x} + \frac{v_{i,j+1}^k - v_{i,j}^k}{\Delta y} \right) \tag{25}$$

The balance equation of momentum (22) is written as:

$$\begin{aligned} \frac{p_{i,j}^{k-1} - p_{i-1,j}^{k-1}}{\Delta x} = & -\frac{2\mu_f}{\Delta x}\left(\frac{u_{i+1,j}^k - u_{i,j}^k}{\Delta x} - \frac{u_{i,j}^k - u_{i-1,j}^k}{\Delta x} \right) \\ & -\frac{\mu_f}{\Delta y}\left(\left[\frac{u_{i,j+1}^k - u_{i,j}^k}{\Delta y} + \frac{v_{i,j+1}^k - v_{i-1,j+1}^k}{\Delta x} \right] - \left[\frac{u_{i,j}^k - u_{i,j-1}^k}{\Delta y} + \frac{v_{i,j}^k - v_{i-1,j}^k}{\Delta x} \right] \right) \\ & +\frac{r_1}{\Delta x}\left(\frac{u_{i+1,j}^k - u_{i,j}^k}{\Delta x} + \frac{v_{i,j+1}^k - v_{i,j}^k}{\Delta y} - \frac{u_{i,j}^k - u_{i-1,j}^k}{\Delta x} - \frac{v_{i-1,j+1}^k - v_{i-1,j}^k}{\Delta y} \right) \\ & +\frac{\mu_f H(\psi_{i,j})}{K_s} u_{i,j}^k \end{aligned} \tag{26}$$

$$\begin{aligned}\frac{p_{i,j}^{k-1}-p_{i,j-1}^{k-1}}{\Delta y} = & -\frac{2\mu_f}{\Delta y}\left(\frac{v_{i,j+1}^{k}-v_{i,j}^{k}}{\Delta y}-\frac{v_{i,j}^{k}-v_{i,j-1}^{k}}{\Delta y}\right) \\ & -\frac{\mu_f}{\Delta x}\left(\left[\frac{u_{i+1,j}^{k}-u_{i+1,j-1}^{k}}{\Delta y}+\frac{v_{i+1,j}^{k}-v_{i,j}^{k}}{\Delta x}\right]-\left[\frac{u_{i,j}^{k}-u_{i,j-1}^{k}}{\Delta y}+\frac{v_{i,j}^{k}-v_{i-1,j}^{k}}{\Delta x}\right]\right) \\ & +\frac{r_1}{\Delta y}\left(\frac{u_{i+1,j}^{k}-u_{i,j}^{k}}{\Delta x}+\frac{v_{i,j+1}^{k}-v_{i,j}^{k}}{\Delta y}-\frac{u_{i+1,j-1}^{k}-u_{i,j-1}^{k}}{\Delta x}-\frac{v_{i,j}^{k}-v_{i,j-1}^{k}}{\Delta y}\right) \\ & +\frac{\mu_f H(\psi_{i,j})}{K_s}u_{i,j}^{k}\end{aligned} \tag{27}$$

The linear system of equations (26)-(27) is solved numerically with an iterative Bi-Conjugate Gradient Stabilized algorithm (BiCGSTAB) [26, 29]. This algorithm is particularly effective for managing the computer memory, because it does not require building and storing the matrix.

4.3 The shear stress at the interface

It is necessary to estimate the tangential stress τ at the interface (cf (8)) numerically. This stress is continuous across the interface, but the velocity vanishes in the soil, and the numerical estimation of the velocity gradient can be difficult. In order to obtain an accurate estimation of the shear stress, it is computed with the fluid velocity only (on the fluid side on the interface), by extending this velocity in several cells in the soil near the interface, as in the "ghost-fluid" method [12].

To improve accuracy, we propose a better approximation of the shear stress at the interface. As the velocity gradient is naturally computed at the center $X_{i,j}$ of the cell and not at the interface, the shear stress module τ is computed at this point and extrapolated on the interface, by using:

$$\tau(X_{i,j}-\psi_{i,j}\nabla\psi_{i,j}) \approx \tau(X_{i,j})-\psi_{i,j}\nabla\psi_{i,j}.\nabla\tau \tag{28}$$

Bearing in mind that ψ is a signed distance to the interface, it is easy to check that $X_{i,j}-\psi_{i,j}\nabla\psi_{i,j}$ is located on the interface.

4.4 The erosion solver

The transport equation (13) is approached numerically by an explicit formulation with respect to a fictitious time and the celerity in vicinity of the interface is extended. Then the transport equation

(11) is approached by an explicit formulation with respect to time under the Courant-Friedrichs-Lewy stability condition (cfl). The resolution of both equations are similar, thus we present only the application of the method to (11). In order to gain accuracy and ensure less diffusion of the interface, a fourth-order Runge-Kutta scheme is used, corresponding to the four following steps:

$$\begin{aligned} k_1 &= \mathbf{c}\cdot\nabla\psi_n \ , \quad \psi^{(2)} = \psi_n + \frac{\delta t}{2}k_1 \\ k_2 &= \mathbf{c}\cdot\nabla\psi^{(2)} \ , \quad \psi^{(3)} = \psi_n + \frac{\delta t}{2}k_2 \\ k_3 &= \mathbf{c}\cdot\nabla\psi^{(3)} \ , \quad \psi^{(4)} = \psi_n + \delta t\ k_3 \\ k_4 &= \mathbf{c}\cdot\nabla\psi^{(4)} \ , \quad \psi_{n+1} = \psi_n + \frac{\delta t}{6}\left(k_1 + 2k_2 + 2k_3 + k_4\right) \end{aligned} \tag{29}$$

In this part, we focus on the terms of type $\mathbf{c}\cdot\nabla\psi$ in (29). We use a finite difference scheme in all space directions. For the sake of simplicity, only the 2D case is described.

In order to avoid numerical dissipation, a high order approximation is used for evaluating the components of the gradient of the Level Set function. We use the fifth order Weighted Essentially Non Oscillatory formulation (WENO 5) [17]. In this formulation, the partial derivative with respect to *x* is computed in two different ways. The first is defined as follows:

$$\partial_x^+\psi_{i,j} = \frac{w_1}{6}\left(2a_1 - 7a_2 + 11a_3\right) + \frac{w_2}{6}\left(-a_2 + 5a_3 + 2a_4\right) + \frac{w_3}{6}\left(2a_3 + 5a_4 - a_5\right). \tag{30}$$

where

$$\begin{aligned} w_1 &= \frac{d_1}{d_1+d_2+d_3}\,; \quad w_2 = \frac{d_2}{d_1+d_2+d_3}\,; \quad w_3 = \frac{d_3}{d_1+d_2+d_3} \\ d_1 &= \frac{1}{10}\frac{1}{\left(\alpha+b_1\right)^2}\,; \quad d_2 = \frac{6}{10}\frac{1}{\left(\alpha+b_2\right)^2}\,; \quad d_3 = \frac{3}{10}\frac{1}{\left(\alpha+b_3\right)^2}\ ; \quad \alpha = 10^{-6} \end{aligned} \tag{31}$$

$$\begin{aligned} b_1 &= \frac{13}{12}(a_1 - 2a_2 + a_3)^2 + \frac{1}{4}(a_1 - 4a_2 + 3a_3)^2 \\ b_2 &= \frac{13}{12}(a_2 - 2a_3 + a_4)^2 + \frac{1}{4}(a_2 - 4a_4)^2 \\ b_3 &= \frac{13}{12}(a_3 - 2a_4 + a_5)^2 + \frac{1}{4}(3a_3 - 4a_4 + a_5)^2 \end{aligned} \tag{32}$$

and for k=1,..,5

$$a_k = \frac{\psi_{i+4-k,j} - \psi_{i+3-k,j}}{\Delta x}. \tag{33}$$

The second $\partial_x^- \psi_{i,j}$ is defined in a quite similar way, by replacing (33) in

$$a_k = \frac{\psi_{i-3+k,j} - \psi_{i-4+k,j}}{\Delta x}. \tag{34}$$

The two values of the derivative with respect to *y*, $\partial_y^- \psi_{i,j}$ and $\partial_y^+ \psi_{i,j}$ are defined in a similar way.

An upwind scheme is used to solve the transport equation avoiding instabilities. This consists in using one or the other value of the partial derivatives depending on the direction of the celerity:

$$\left(\mathbf{c} \cdot \nabla\right)\psi\Big|_{i,j} = \max(c_{i,j}^x, 0)\partial_x^+ \psi_{i,j} + \min(c_{i,j}^x, 0)\partial_x^- \psi_{i,j} + \max(c_{i,j}^y, 0)\partial_y^+ \psi_{i,j} + \min(c_{i,j}^y, 0)\partial_y^- \psi_{i,j} \tag{35}$$

where $c_{i,j}^x$ and $c_{i,j}^y$ stand for the components of **c**.

The algorithms described above give the new value ψ_{n+1} of the Level Set. Due to singularities, in particular when extending the celerity of the interface, the computation of ψ_{n+1} is accurate only in the vicinity of the interface. This is not a problem if the sign of ψ_{n+1} (or $H\left(\psi_{n+1}\right)$) is well defined. An accumulation of errors during the numerical process may lead to ψ functions whose level sets are difficult to determine. To avoid this problem, we modify ψ_{n+1} when necessary, without changing its zero level set Γ, by reinitializing it as the signed distance to Γ. Sussman [27] proposed an iterative scheme for this step called "redistancing". Once again, the main idea is to solve a fictitious PDE problem:

$$\begin{cases} d(\mathbf{x}, t, t^* = 0) = \psi_{n+1}(\mathbf{x}, t) \\ \dfrac{\partial d}{\partial t^*} + \mathrm{sgn}(\psi_{n+1})\left[\left\|\nabla d\right\| - 1\right] = 0 \end{cases} \tag{36}$$

where t^* is a fictitious time and $\mathrm{sgn}(\psi)$ is equal to 1 if $\psi > 0$ and *-1* elsewhere. The redistancing step consists in replacing ψ_{n+1} by solution *d* of this problem.

5 RESULTS

5.1 Erosion of a soil cylinder

We consider a simple test case: the erosion of a fixed cylinder of soil in a channel (Figure 4) (radius 0.3 m, length 2 m, height 1 m, mesh 200x100). We impose a pressure gradient from the left to the right and a wall condition on the top and the bottom of the domain (ρ_f=1000 kg/m^3, μ_f=0.001 Pa/s, k_{er}=0.001 s/m, τ_c=10-20 Pa, r_1=r_2=1, cfl=0.8, δP=0.1 Pa).

Figure 5 shows the evolution of the cylinder due to erosion. We then verify that, as expected, the shape and the flow are symmetrical, and that the cylinder is mostly eroded at its upper and lower parts. Figure 6 shows that accuracy is greatly improved when comparing the evolution of the shape of the cylinder with or without the shear stress extrapolation at the interface, defined by (28). As the interface is described more accurately, function ψ is smoother and fewer redistancing processes are needed, thereby improving both accuracy and computation time.

5.2 Hole erosion test

We consider a sample of soil in which a small cylindrical hole has been made (Figure 7). A fluid flow is then imposed in the hole in such way that an erosion process increases the radius of the cylinder. This situation corresponds to the “Hole Erosion Test” and was studied in the case of a turbulent piping flow [3, 19]. Here, we focus on a laminar flow.

It is possible to compare the numerical simulation to the analytical solution developed by [3]. These authors propose the following law for flow rate *Q* and the evolution of radius *R*, where δP denotes the imposed pressure gradient, R_0 the initial radius and *L* the length of the sample.

$$Q(t) = \frac{\pi\ \delta P\ R^4(t)}{8\mu_f L} \tag{37}$$

$$R(t) = \frac{2L\tau_c}{\delta P} + \left(R_0 - \frac{2L\tau_c}{\delta P}\right)\exp\left(\frac{k_{er}\delta P}{2L\rho_s}\ t\right) \tag{38}$$

Good agreement (the better when the mesh is refined) can be observed when comparing the evolution of radius versus time (Figure 8) and the evolution of the flow rate versus radius (Figure 9).

In the three-dimensional case (Figure 10), we verify that axisymmetry is preserved until the interface reaches the boundary of the domain. As in the previous case, Figures 8 and 9 show that using (28) significantly increases accuracy.

5.3 Erosion around a bridge

Soil erosion around a bridge pier is considered in a full three-dimensional case. A wall condition is applied at the bottom of the computational box, a symmetric condition at its top, a periodic condition at the sides and a pressure gradient is imposed between the inlet and the outlet. A coarse mesh 150x50x50 is used since it is simply a prospective case. Obviously, a more realistic simulation would need to take into account a free surface and a turbulent flow, but this is out of the scope of this study.

Two level Set functions are used: one for the interface with the bridge pier, which is assumed to be a non erodible material, and another for the soil-fluid interface. The erosion process stops as soon as the shear stress at the interface falls below the threshold shear stress. This numerical simulation requires about 2 days on a standard PC, thereby proving the feasibility of such 3D simulations.

6 CONCLUSION

The aim of this study was to draw up a numerical model for simulating interfacial erosion due to tangential flows. We presented an erosion process with a unified model using a penalization procedure (fictitious domain method) that permits avoiding prohibitive remeshing methods. The water/soil interface evolution was described by a Level Set function. A finite volume formulation

was developed on a Cartesian MAC mesh to approximate the flow, in order to allow the use of appropriate fast solvers. The ability of the model to predict the interfacial erosion of soils was confirmed by several illustrative examples. Our model can be enhanced but at the price of increased complexity and thus computational cost.

Acknowledgment: This work was funded by the Région Provence Alpes Côte d'Azur and by the French National Research Agency (ANR) through the COSINUS program (project CARPEINTER n°ANR-08-COSI-002). The authors wish to thanks Professor Cédric Galusinski for his valuable advice.

REFERENCES

[1] Angot P., Bruneau, C.-H. & Fabrie, P., A penalization method to take into account obstacles in incompressible viscous flows, Numer. Math., Vol. 81, 497-520, 1999.

[2] Angot P., Analysis of Singular Perturbations on the Brinkman Problem for Fictitious Domain Models of Viscous Flows, Math. Meth. Appl. Sci., 22, 1395-1412, 1999.

[3] Bonelli, S., Brivois, O., The scaling law in the hole erosion test with a constant pressure drop, Int. J. Num. Meth. Eng., Vol. 32, 1573-1595, 2008.

[4] Bost C., Cottet G.-H., Maitre E., Numerical analysis of a penalization method for the three-dimensional motion of a rigid body in an incompressible viscous fluid, submitted, arXiv:0901.1958.

[5] Brivois, O., Bonelli, S., Borghi, R., Soil erosion in the boundary layer flow along a slope: a theoretical study, Eur. J. Mech. B-Fluid., Vol. 26, 707-719, 2007.

[6] Chang Y.C., Hou T.Y., Merriman B., Osher S., A Level Set formulation of eulerian interface capturing methods for incompressible fluid flows, j. comp. phys., 124, 449-464, 1996.

[7] Chantalat F., Bruneau C.H., Galusinski C., Iollo A., Level-set, penalization and cartesian meshes: A paradigm for inverse problems and optimal design, j. comp. phys., 228, 6291-6315, 2009.

[8] Chauchat J., Médale M., A three-dimensional numerical model for incompressible two-phase flow of a granular bed submitted to a laminar shearing flow, Computer Methods in Applied Mechanics and Engineering, 199 (9-12), 439-449, 2010.

[9] Chorin A.J., A Numerical Method for Solving Incompressible Viscous Flow Problems, J. of Comp. Phys., 2 (1), 12-26, 1967.

[10] Christakis N., Allsop N.W. H., Beale R.G., Cooper A. J., Dennis J. M., A volume of fluid numerical model for wave impacts at coastal structures, Proceedings of the Institution of Civil Engineers Water & Maritime Engineering, Issue 3, Pages 159-168, 2002.

[11] Diaz-Goano C., Minev P.D., Nandakumar K., A fictitious domain/finite element method for particulate flows, j; of comp. phys., 192, 105-123, 2003.

[12] Fedkiw, R., "Coupling an Eulerian Fluid Calculation to a Lagrangian Solid Calculation with the Ghost Fluid Method", J. Comput. Phys. 175, 200-224, 2002.

[13] Fortin M., Glowinski R., Augmented lagrangian methods: applications to the numerical solution of boundary-value problems, studies in mathematics and its applications, vol. 15, North-Holland, Amsterdam, 1983.

[14] Galusinski C., Vigneaux P., On stability condition for bifluid flows with surface tension: application to microfluidics, J. of Comp. Phys., 227, 6140-6164, 2008.

[15] Golay F., Lachouette D., Bonelli S., Seppecher P., Interfacial erosion: A three-dimensional numerical model, C.R. Mecanique, to appear, 2010.

[16] Harlow FH, Welsh JE. Numerical calculation of time dependent viscous incompressible flow with free surface., Phys Fluids, 8 (12), 2182–2189, 1965.

[17] Jiang, G.S. & Peng, D., Weighted ENO schemes for Hamilton-Jacobi equations, J. Sci. Comput., Vol. 21(6), 2126-2143, 2000.

[18] Khadra K., Angot P., Parneix S., Caltagirone,J.P., Fictitious domain approach for numerical modelling of Navier-Stokes equations, Int. J. Numer. Meth. Fluids, 34, 651-684, 2000.

[19] Lachouette, D., Golay, F., Bonelli, S., One-dimensional modeling of piping flow erosion, C. R. Mecanique, Vol. 336, 731-736, 2008.

[20] Olson E., Kreiss G., A conservative level set method for two phase flow, j. comp. phys., 210, 225-246, 2005.

[21] Osher, S., Sethian, J.A., Fronts propagating with curvature-dependent speed: Algorithms for tracking material interface, J. Comp. Phys., Vol. 39, 201-225, 1981.

[22] Papamichos E, Vardoulakis I, Tronvoll J, Skjaerstein A. Volumetric sand production model and experiment. Int. J. Num. Anal. Meth. Geomechanics; **25**, 789-808, 2001.

[23] Patil P. P., Tiwari S., Computation of flow past complex geometries using MAC algorithm on body-fitted coordinates, Eng. App. of Comp. Fluids Mech, 3 (1), 15-27, 2009.

[24] Prodanovic M., Bryant S., A level set method for determining critical curvatures for drainage and imbibition, j. colloid and int. Sci., 304, 442-458, 2006.

[25] Ramiere I., Angot P., Belliard M., A fictitious domain approach with spread interface for elliptic problems with general boundary conditions, comp. meth. In app. Mech. Eng., 196, 4-6, 766-781, 2007.

[26] Sleijpen G., Fokkema D., Bicgstab(L) for linear equations involving unsymetric matrices with complex spectrum, Elec. Trans. on Num. Ana., 1, 11-32, 1993.

[27] Sussman, M., Smereka, P., Osher, S., A level set approach for computing solutions to incompressible two-phase flows, journal of Computational physics, 114:146-159, 1994.

[28] Temam R. , Une méthode d'approximation de la solution des équations de Navier-Stokes, Bull. Soc. Math. France, 96, 115-152, 1968.

[29] Van der Vorst H., Bi-CGSTAB : a fast and smoothly converging variant of Bi-cg for the solution of nonsymetric linear systems, SIAM J. Sci. Stat. Comp., 13(2), 631-664, 1992.

[30] Vardoulakis I, Stavropoulou M, Papanstasiou P. Hydromechanical aspects of sand production problem. Transport in Porous Media; **22**, 225-244, 1996.

[31] Vardoulakis, I., Papanastasiou, P. & Stavropoulou, M., Sand Erosion in Axial Flow Conditions, Transport Porous Media, Vol. 45, 267–281,2001.

[32] Vigneaux P., Méthodes Level Set pour des problèmes d'interface en microfluidique, PhD thesis, university of Bordeaux I, 2007.

[33] Vincent S., Modélisation d'écoulements incompressibles de fluides non-miscibles, PhD thesis, university of Bordeaux, France, 1999.

[34] S. Vincent, J.P. Caltagirone, A One-cell local multigrid method for Solving unsteady incompressible multiphase flows, J. Comp. Phys., 163, 172-215, 2000.

[35] S. Vincent, J.P. Caltagirone, P. Lubin and T. N. Randrianarivelo, An adaptative augmented Lagrangian method for three-dimensional multimaterial flows, Comp. Fluids, 33 (10), 1273-1289, 2004.

LIST OF FIGURE CAPTIONS

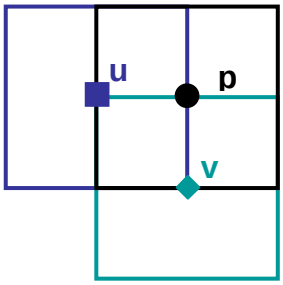

Figure 1. The MAC mesh

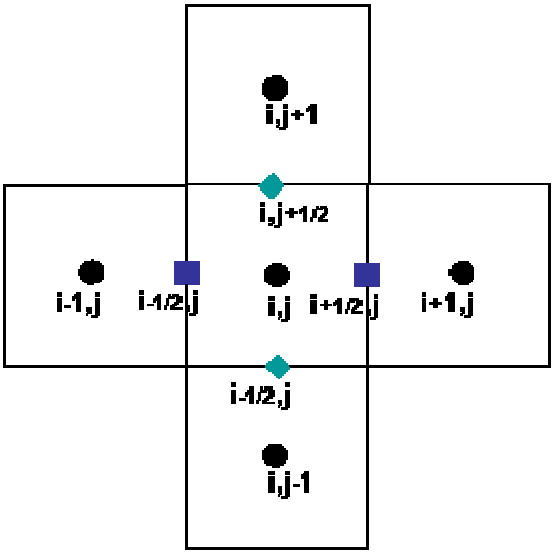

Figure 2. The subscripts of the staggered grid

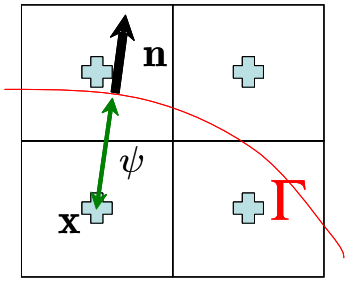

Figure 3. Extrapolation of the shear stress from center **x** to interface Γ.

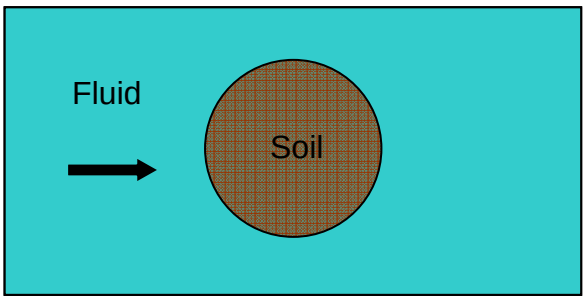

Figure 4: Erosion of a cylinder

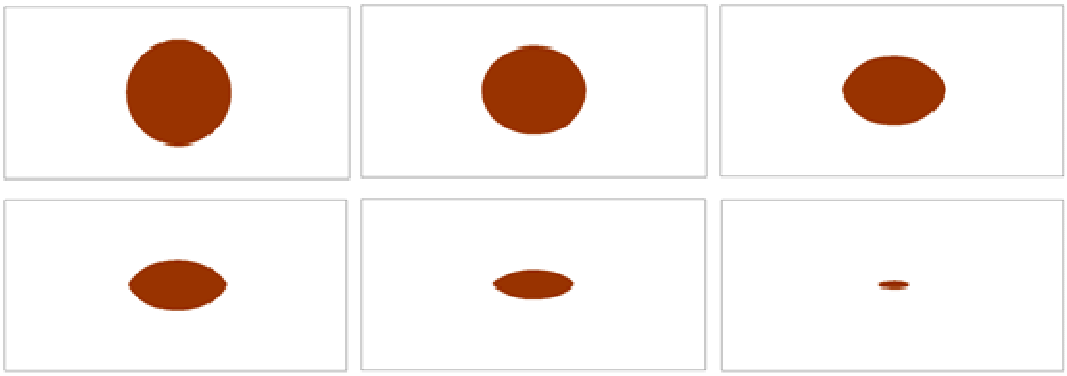

Figure 5: Evolution of the shape of the cylinder through time: t=0, 0.5, 1., 1.5, 2., 2.4 Ms

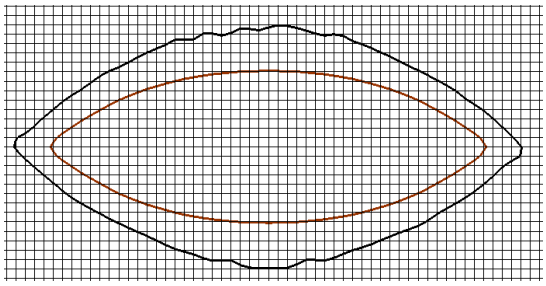

Figure 6: Shape of the cylinder at t=2Ms, without (black line) and with (brown line) extrapolation of the shear stress (eq. (28))

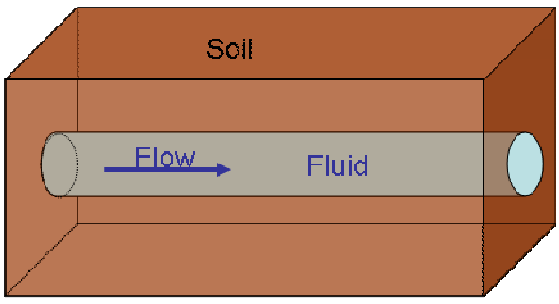

Figure 7: The Hole Erosion Test

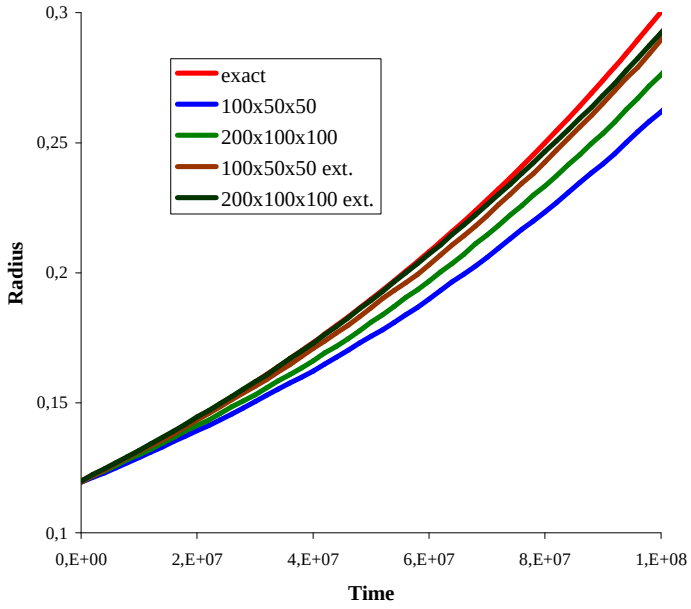

Figure 8: Evolution of the radius through time

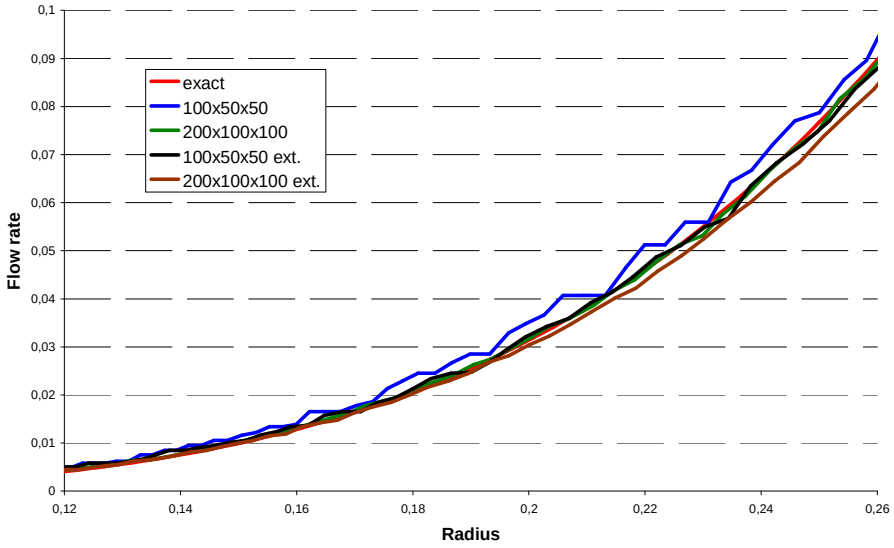

Figure 9: Evolution of the flow rate as the radius increase

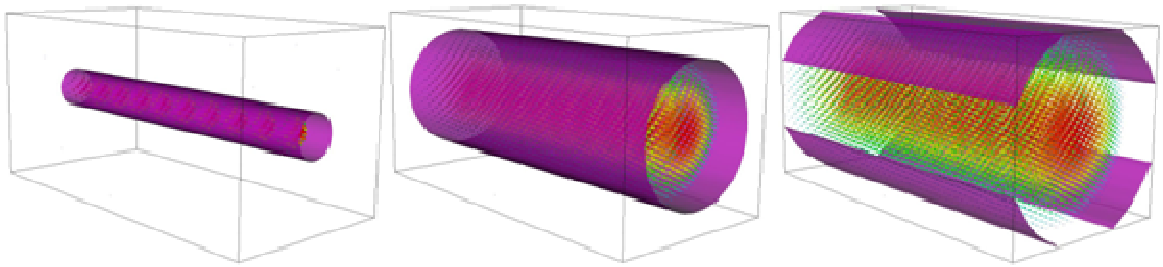

Figure 10: Evolution of the initial and intermediate interface as the computation boundary is reached

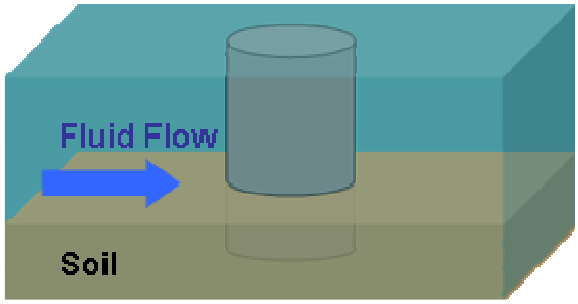

Figure 11: Erosion around a bridge pier

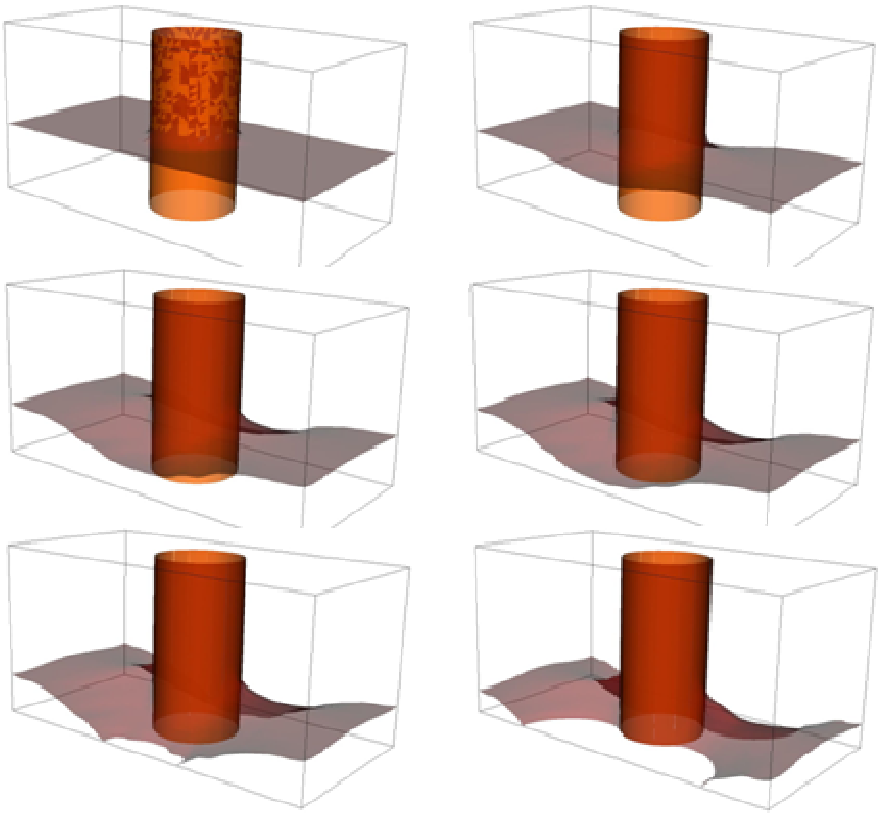

Figure 12: Erosion around a bridge pier at t=0., 19., 42., 55., 66., 95. Ms